Diffusion-Assisted Formation Mechanism of Molecular Break Junctions: A First-Principles Study of Benzenethiolate on Au(111)

ARTICLE *in* THE JOURNAL OF PHYSICAL CHEMISTRY C · FEBRUARY 2011

Impact Factor: 4.77 · DOI: 10.1021/jp110072w

2 AUTHORS, INCLUDING:

Vidvuds Ozolins

University of California, Los Angeles

179 PUBLICATIONS **4,084** CITATIONS

THE JOURNAL OF PHYSICAL CHEMISTRY C

ARTICLE

pubs.acs.org/JPCC

Diffusion-Assisted Formation Mechanism of Molecular Break Junctions: A First-Principles Study of Benzenethiolate on Au(111)

Yongduo Liu and Vidvuds Ozolins*

Department of Materials Science and Engineering, University of California, Los Angeles, California 90095-1595, United States

ABSTRACT: Density-functional theory (DFT) calculations have been used to obtain the binding energies of benzenethiolate on Au(111) under applied stress. The binding energetics to ideal Au(111), as well as to Au adatoms and small 2−3 adatom islands, have been calculated as functions of the normal displacement applied to the free end of the molecule. We find that binding to adatoms and adatom islands is energetically preferred over breaking the Au−S bond for sufficiently large displacements. On the basis of these results, we propose a diffusion-assisted mechanism of pyramidal break junction formation on Au(111) that involves creation and capture of surface adatoms, as well as surface or bulk vacancies. Quantitative estimates of stretching rates that are compatible with the required diffusion times are given on the basis of random walk theory.

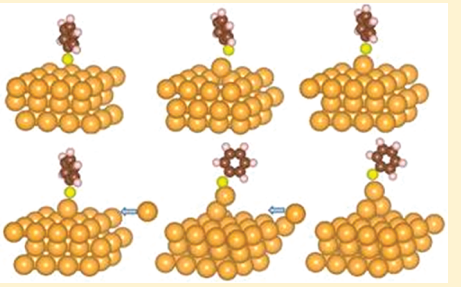

I. INTRODUCTION

Ever since the first molecular bridge junctions were made and reported in 1997,[1] molecular electronics has been a rapidly growing field promoted by today's single-molecule manipulation techniques and by prospective technological applications in switches, rectifiers, transistors, and memory devices.[2−6] Most of the potential applications are based on charge transport properties of individual organic molecules, which are commonly investigated by trapping molecules in break junctions and measuring their current−voltage characteristics.[1] These break junctions can be obtained by a number of different methods, e.g., by bending and breaking a metal wire[1] or by direct lithography.[7] A commonly used and widely studied type of break junction is formed by the tip of a scanning tunneling microscope (STM) and gold substrate serving as two electrodes with a molecule between them bridging the junction electronically.[8,9] Recently, several studies have investigated amine- or thiolate-anchored molecular junctions by pulling up the Au STM tip and measuring the tunneling current and conductance during junction stretching.[10,11] One of the electrodes can also be heated to apply a temperature difference and measure the value of the molecular Seebeck coefficient.[8] In addition, numerous computational studies have been carried out to calculate the conductance of molecular junctions.[12,13]

It is well-known that electronic transmission coefficients are very sensitive to the structure of the contact between the molecule and the metal electrode. For instance, it has been shown that the S−Au bond and the atomic geometry of the connection significantly influence charge transport through the molecule and therefore determine switching properties.[14] However, the morphology and formation mechanisms of Au−thiolate contacts are not yet fully understood. A recent molecular dynamics (MD) simulation using Au clusters by Li[12] has shown that there is a significant geometrical distortion of the Au electrode when a pulling force is applied to the thiolate-anchored junction, but a quantitative description on this phenomenon was not given. Rupture of a 6-mercapto-1-hexanol molecule on ideal Au(111) under normal or parallel stretch has been studied by Wang et al.[15] using first-principles density-functional theory (DFT) calculations; these authors reported that normal stretching can cause one Au atom to become separated from the surface, and the junction could be ruptured by applying a force of a few nanoNewton. The Au−thiolate system is also a prototype for a variety of studies in self-assembled monolayers (SAMs),[16] with the Au(111) surface being the most widely used.[17,18] Currently, it is thought that the sulfur end groups are bonded to surface inhomogeneities, such as adatoms, vacancies, islands, or step edges,[18−20] but an in-depth understanding of the binding geometries and energies is still lacking.

In this paper, we use first-principles density-functional theory (DFT) calculations to investigate the changes in the morphology of Au(111) electrodes during junction stretching. We calculate the binding energies of a single thiolate molecule on ideal Au(111), as well as of Au adatoms and small 2−3 adatom Au islands on Au(111) as functions of normal displacement applied to the free end of the molecule. On the basis of the calculated energetics and surface structures, we propose a diffusion-assisted mechanism for the formation of pyramidal break junctions during morphological evolution under applied stress.

II. COMPUTATIONAL METHODS

Density-functional theory (DFT) calculations were performed using the Vienna Ab Initio Simulation Package (VASP)[21] and the Perdew−Burke−Ernzerhof (PBE)[22] form

Received: October 20, 2010
Revised: January 4, 2011

   dx.doi.org/10.1021/jp110072w | J. Phys. Chem. C XXXX, XXX, 000–000

Table 1. Convergence Test for the Adsorption Energy ΔE_{ads} of the SH Molecule on Ideal Au(111) Using Equivalent k Point Meshes

surface supercell	k point mesh	ΔE_{ads} (eV)
3 × 3	4 × 4	2.34
4 × 4	3 × 3	2.25
6 × 6	2 × 2	2.26

Table 2. Convergence of Adatom Formation Energy ΔE_{adatom} on Ideal Au(111)[a]

	cell size	k point mesh	ΔE_{adatom} (eV)
this work	3 × 3	2 × 2	0.679
	3 × 3	4 × 4	0.605
	3 × 3	6 × 6	0.653
	3 × 3	8 × 8	0.620
other DFT	3 × 3	8 special k points	0.670
exptl.[25]	–	–	0.685

[a] The formation energy is defined as the energy difference between the adatom on Au(111) and energy per atom of bulk Au.

of the generalized gradient approximation (GGA). The electron−core interactions were described by ultrasoft pseudopotentials[23] using $1s^1$, $2s^22p^2$, $3s^23p^4$, and $6s^15p^05d^{10}$ valence configurations for H, C, S, and Au, respectively, and wave functions were expanded in a plane-wave basis set with a cutoff energy of 300 eV. The calculated bulk lattice parameter of Au, $a = 4.18$ Å, agrees well with earlier studies[24] and was kept fixed during our surface slab calculations. The Au(111) surface was modeled as a slab of six layers of Au and seven layers of vacuum with periodic boundary conditions applied in all three dimensions. Molecules were adsorbed on top of the slab, and the bottom two layers of the slab remained fixed. The coordinates of the third layer from the bottom were fixed in the horizontal direction, and all other atoms are relaxed until the forces were less than 0.01 eV/Å. A 3 × 3 surface supercell was used to represent a single adsorbed molecule, and the surface Brillouin zone was sampled on a 4 × 4 mesh of **k** points. Extensive convergence tests with larger cells and equivalent **k** point meshes were performed for sulfur−hydrogen group (SH) adsorption energies and adatom formation energies on Au(111) to validate our choices. As shown in Table 1, the 3 × 3 surface supercell yields convergence of the SH/Au(111) adsorption energies to better than 0.1 eV, which is sufficiently accurate for the aims of the present study (and likely significantly lower than the expected error due to the approximate nature of the PBE functional). The calculated adatom formation energy (as shown in Table 2) exhibits oscillating convergence with respect to the number of **k** points, slowly converging to approximately 0.63 eV. This behavior is likely caused by electronic Friedel oscillations on Au(111) due to the presence of the adatom. Our choice of supercell and **k** point mesh results in an adatom energy error of only 20−30 meV, which is well within the error tolerance of the current work. We also note here that the energy differences between different surface configurations obtained using the same surface supercell and **k** point mesh are expected to be significantly more accurate than the adsorption energies and adatom formation energies in Tables 1 and 2 due to the cancellation of systematic errors.

It is an experimentally well-established fact that the dissociative adsorption happens when the thiol molecule bonds to the Au(111) surface.[26] The energy needed to detach the S−H bond is more than compensated by the formation of the S−Au bond and the hydrogen molecule. At very low temperatures (less than −150 °C), the dissociative reaction may be kinetically inhibited, but at room temperature and above the adsorption is always dissociative. Therefore, in this work, we use C_6H_5S and only consider the dissociative adsorption.

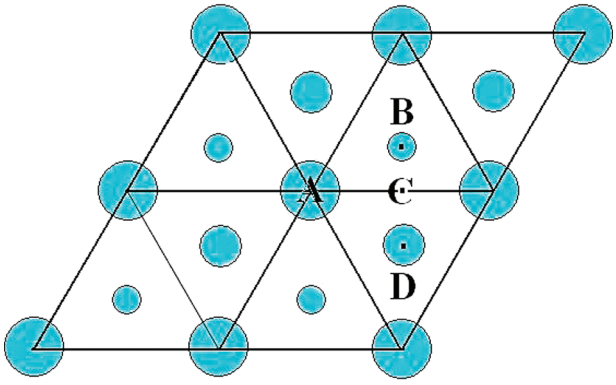

Figure 1. Possible adsorption sites for C_6H_5S on Au(111). Large, medium, and small circles represent Au atoms in the 1st, 2nd, and 3rd surface layers, respectively.

III. RESULTS AND DISCUSSION

III.A. Adsorption on Ideal Au(111). We begin by determining the energetically favored adsorption site for C_6H_5S on Au(111). Configurations with the sulfur ion in on-top, bridge, and hollow sites are chosen as starting points, which are subsequently relaxed to find the local energy minima and optimized structures (Figure 1). Table 3 shows our results and compares them with the results of a previous DFT study by Nara et al.[27] We find that the bridge site is favored energetically, in agreement with ref 27. We also find that the configuration with the molecule in the hollow site relaxes to the bridge site during structural optimization. The on-top site is metastable but has the highest energy.

We also study the binding properties between thiolates and gold adatoms by calculating the following quantities

$$E'_A = E_{C_6H_5S/Au(111)} - E_{Au(111)} \quad (1)$$

and

$$E'_B = E_{C_6H_5S-Au/Au(111)} - E_{Au/Au(111)} \quad (2)$$

where $E_{C_6H_5S/Au(111)}$ is the energy of a perfect surface with an adsorbed molecule; $E_{C_6H_5S-Au/Au(111)}$ is the energy of a system with a molecule adsorbed on top of an adatom; $E_{Au(111)}$ is the energy of a perfect Au(111) surface; and $E_{Au/Au(111)}$ is the energy of Au(111) with an adatom. The difference $E'_A - E'_B$ represents the binding energy between the thiolate molecule and an isolated Au adatom. At ground state, we obtain a binding energy of 0.2 eV, which indicates that it is much more favorable for a molecule to bond to a pre-existing adatom than to a clean Au(111) surface, but the binding energy is not sufficient to compensate for the energy cost of converting a bulk Au atom into an adatom (0.62 eV, see Table 2). This result agrees qualitatively with the results of previous experimental investigations of self-assembled monolayers (SAM) of thiolates on Au(111), which have shown that the

dx.doi.org/10.1021/jp110072w |J. Phys. Chem. C XXXX, XXX, 000–000

Table 3. Calculated Adsorption Energies and Tilting Angles for C_6H_5S on Au(111)[a]

	ΔE_{ads} (eV)		Tilting angle	
adsorption site	current work	ref 27	current work	ref 27
bridge	1.54	1.37	60.6	60.9
fcc-hollow	unstable	1.27	n/a	19.9
hcp-hollow	unstable	1.18	n/a	21.1
on-top	1.29	1.05	76.0	79.4

[a] The tilting angle is defined as the angle between the S−C bond and the surface normal.

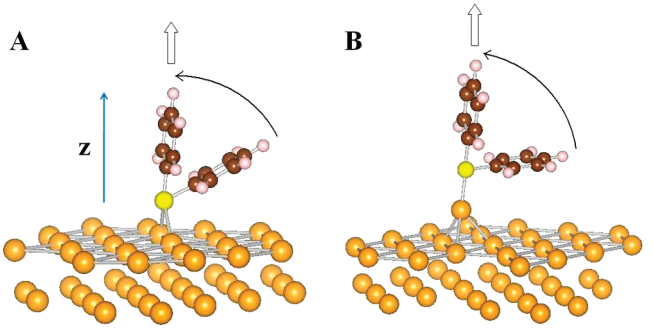

Figure 2. Schematic illustration of two sets of calculations used to study molecule−surface interactions: (A) bonding of benzenethiolate to perfect Au(111) and (B) bonding of benzenethiolate to a gold adatom on Au(111).

sulfur end group of a thiolate often bonds to Au adatoms that are created by adsorption-induced lifting of the Au(111) surface reconstruction.[28] For instance, several studies have observed structures where sulfur binds to the top of an adatom or forms a dumbbell-like complex with one adatom and another thiolate molecule.[19,29]

III.B. Behavior of Benzenethiolate under Normal Stretch.

After establishing the favored binding site for C_6H_5S/Au(111), we discuss the binding properties between the benzenethiolate and Au(111) under applied mechanical stress. For reasons of computational efficiency, we use 1-benzenethiolate C_6H_5S as a substitute for 1,4-dithiolate, $S2C_6H_6$, which is commonly used in experimental studies of molecular junctions.[8] The experimental conditions of pulling force applied to the end of the molecule are simulated here by fixing the position of the hydrogen atom at the para site of the benzene ring at different heights relative to the Au(111) substrate; this hydrogen atom can move freely in the direction parallel to the surface. To take into account changes in the surface structure under applied stress, we carry out two sets of calculations. The first set of calculations is performed using the benzenethiolate on ideal Au(111) with the ground state of the molecule as the starting configuration (bridge-site with 60 tilting-degrees). The molecule is then gradually flipped up and pulled upward, as shown in Figure 2A. The other set of calculations uses a Au adatom on Au(111) as the bonding site for the benzenethiolate, as illustrated in Figure 2B. In all cases, the molecule is allowed to rotate about the S−C bond.

To present our results quantitatively, we introduce the following quantities

$$E_A = E_{C_6H_5S/Au(111)} \quad (3)$$

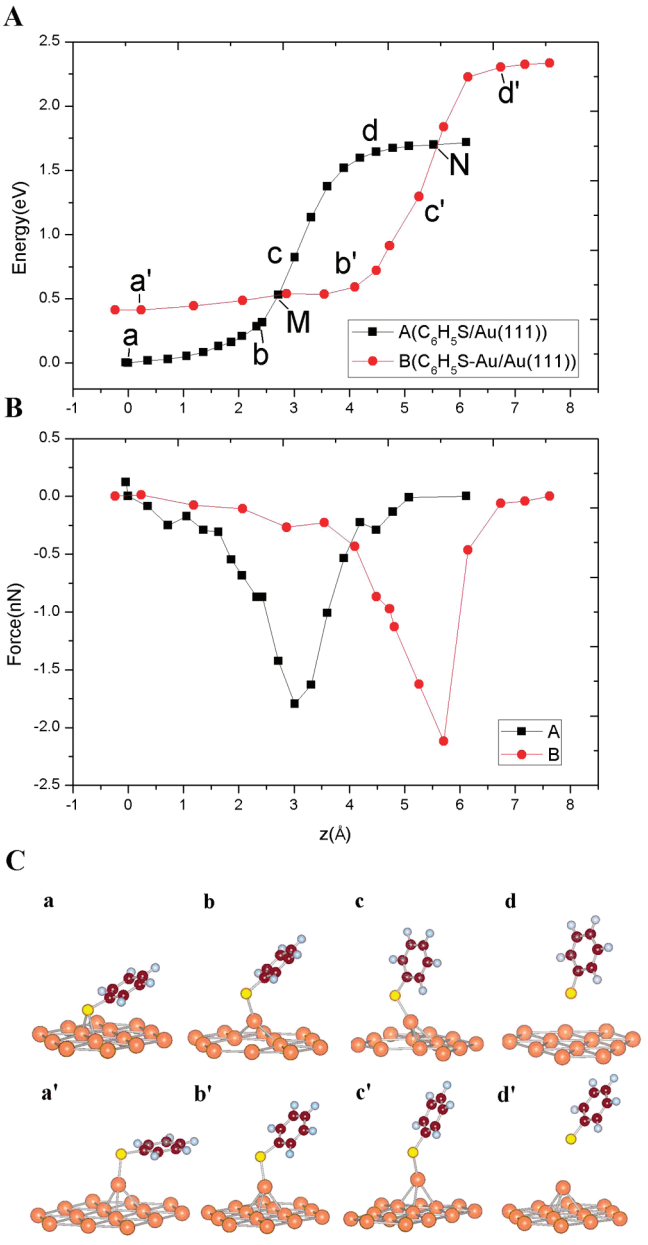

Figure 3. (A) Energies E_A and E_B defined by eqs 3 and 4 versus the z coordinate of the para-site H atom. The z coordinate is referenced relative to the height of the para site hydrogen in the ground state of C_6H_5S on ideal Au(111), and the energy is given relative to the ground state adsorption energy. (B) Forces on the para-site H atom along the direction of the surface normal along the pulling trajectory. (C) Atomic configurations for (a−d) a molecule on clean Au(111) and (a′−d′) bonded to a gold adatom.

and

$$E_B = E_{C_6H_5S-Au/Au(111)} - \mu_{Au} \quad (4)$$

where μ_{Au} is the chemical potential of Au, which we set equal to the bulk energy of fcc Au. Equation 3 represents the energy of a molecule bonded to perfect Au(111), while eq 4 is the energy of a molecule bonded to an adatom, plus the energy cost to convert a bulk Au atom into an adatom. Figure 3A shows the calculated E_A (black symbols) and E_B (red symbols) as functions of the perpendicular coordinate z of the fixed

dx.doi.org/10.1021/jp110072w |J. Phys. Chem. C XXXX, XXX, 000–000

para-site hydrogen atom. If $E_B < E_A$ for some value of z, it is energetically favorable to convert a bulk Au atom into an adatom. In contrast, when $E_A < E_B$, it is energetically favorable to bind to the perfect surface. The two curves in Figure 3A cross at points M and N, showing that binding to perfect Au(111) is favorable at small values of the vertical displacement z, where the molecule is close to its unstrained state, and at very large values of z, where the S−Au bond is broken. Near the ground state (for z below M), bonding to the clean surface is more favorable because the energy gain by bonding between the sulfur and adatom (0.2 eV, see the preceding discussion) is less than the energy cost to generate an adatom (0.62 eV, see Table 2). For vertical displacements between M and N, corresponding to the region of high tensile strain in the Au−S bond, creating an adatom and shortening the sulfur−adatom bond is more favorable than bonding to perfect Au(111). Above the point N in Figure 3A, perfect Au(111) again becomes energetically favorable because the bonding between the sulfur and adatom becomes too weak. Both curves eventually reach plateaus, which correspond to the states where the Au−S bonds are broken, and the offset between the two curves is just the formation energy of a Au adatom.

Further insight into molecule−surface interactions can be gained by analyzing atomic configurations along the pulling trajectories. For the case of thiolate on perfect Au(111) (cf. configurations a−d in Figure 3C), it is apparent that the Au atom, which was initially bonded to the sulfur of the molecule (configuration a in Figure 3C) is pulled out to a significant extent. For instance, in configuration b of Figure 3C, the normal displacement of this Au atom is approximately 1.66 Å, which is slightly more than half of the equilibrium Au−Au distance of 2.95 Å. Upon further displacement, the energy increases sharply as one goes from configuration b to c in Figure 3C, which corresponds to the deformation of the Au−S−C bond angle without significantly changing the positions of the Au surface atoms. Finally, the Au−S bond is severed, and the Au atom retreats back into the surface in configuration d of Figure 3C. Our findings for thiolate on clean Au(111) differ from the results of ref 15, which proposed that one Au atom could become completely separated from the Au surface due to continued stretching of the Au−S bond. We have checked our results by evaluating the energy of the configuration where one Au atom has become detached from the perfect surface (leaving behind a surface vacancy) and is attached to the sulfur of the benzenethiolate. Our results show that this energy is 1.1 eV higher than the energy of configuration d of Figure 3C where the Au−S bond has been severed and the Au atom has retreated back into the surface, restoring the perfect surface. Therefore, we conclude that it is energetically unfavorable to pull a gold atom out of the ideal (111) surface.

Figure 3B shows the normal force exerted on the fixed para-site H atom as a function of its z coordinate. This force has been calculated from the self-consistent DFT wave functions using the Hellmann−Feynman theorem; it could also be obtained from the slope of the energy plot in Figure 3A. The maximum absolute value of the force represents the theoretical yield strength of the Au−S bond. The calculated maximum forces for the ideal Au(111)- and adatom-bonded cases are 1.8 and 2.2 nN, respectively, showing that the Au−S bond is slightly stronger in the latter case. Our calculated forces are in good agreement with another DFT result obtained by Kruger et al.,[20] who calculate

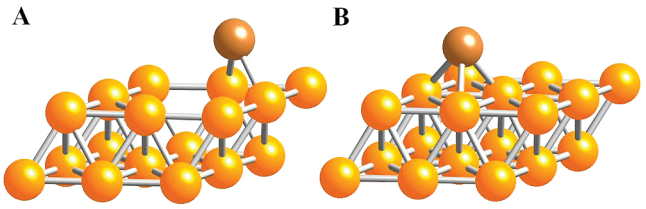

Figure 4. Illustration of the surface atom in Figure 3C c with four of its surface bonds being cut off and the adatom in Figure 3C c′ with its three nearest neighbors.

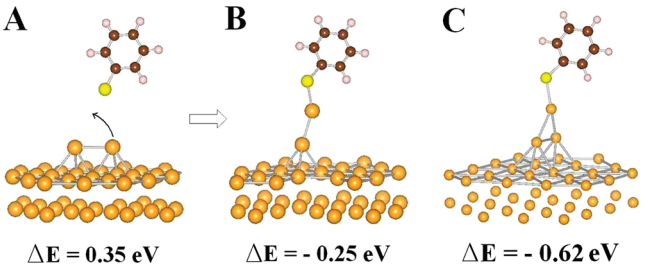

Figure 5. Schematic illustrations of the thiolate molecule bonding to two and three Au adatoms on Au(111). Energies are referenced to the configuration c′ in Figure 3C and to the chemical potential of bulk Au, $\Delta E = E - E(c') - n\mu_{Au}$.

that the rupture force during the pulling process along the ⟨111⟩ direction over a step edge is 1.2 nN. Our results are also in line with the experimental data of approximately 1.4 nN.[30]

For the case of the molecule binding to a surface adatom (see configurations a′ to d′ in Figure 3C), we find only very weak distortions of the Au−Au bond lengths around the adatom in response to the applied force, which is in sharp contrast to the behavior on perfect Au(111). To understand the reason for this difference, we analyze the bond lengths in configurations c and c′ of Figure 3C. Figure 4 gives schematic close-up view of these configurations.

As seen from Figure 4A for thiolate on perfect Au(111), seven of the nine nearest-neighbor bonds have been severed for the displaced surface Au atom (four bonds with atoms in the surface layer and another three with atoms in the subsurface layer). It remains bonded to two of its nearest neighbors at distances 2.71 and 2.75 Å, respectively, which are 10% shorter than the equilibrium Au−Au distance in bulk Au. Our results suggest that the two remaining Au−Au bonds have stiffened considerably due to reduced coordination and increased electronic density along the bonds and that further displacement of the molecule acts to elongate and eventually cut the Au−S bond. In contrast, the adatom is strongly bonded to its three nearest neighbors in the surface layer, and the reduced coordination again leads to enhancement in the stiffness of these bonds when compared to regular metallic bonds in bulk Au. These results show that the Au−Au bond strength is highly dependent on the coordination environment of the surface atoms.[31]

III.C. Bonding to Two- and Three-Adatom Islands. In this section, we study the interaction between the thiolate and small Au islands to gain further insight into the interplay between the surface coordination and interatomic bond strength. We choose the configuration d′ in Figure 3C with the para-site hydrogen fixed at z = 6.2 Å with respect to the ground state position (configuration a′ in Figure 3C) and investigate the energetics of

dx.doi.org/10.1021/jp110072w |J. Phys. Chem. C XXXX, XXX, 000–000

adding another Au adatom in the gap between the sulfur and the Au adatom (see Figure 5B). We also considered the energy of a surface dimer forming below the molecule (see Figure 5A), finding that converting a second bulk Au atom into a surface atom that is not bonded to S requires an energy cost of 0.35 eV. Surprisingly, when the added Au is moved to bridge the gap between the Au adatom and S, the energy gain is 0.6 eV, making the transfer of a Au atom from the bulk to the surface energetically favorable by 0.25 eV. When taken together with Figure 3A showing that conversion of bulk atoms into surface adatoms becomes energetically favored for sufficiently large displacements, these results show that two bulk Au atoms can be converted into a monatomic nanowire during the stretching process, preventing the rupture of the S−Au bond. Further insight into nanowire formation can be reached by considering three adatoms in Figure 5C, which is obtained from the two-adatom configuration in Figure 5B by adding a third Au atom to the bridge site of the two-adatom island. We again find that the conversion of a bulk Au into a surface adatom is energetically favorable by 0.6 eV, so that the three-adatom configuration is energetically favored over the one- and two-adatom configurations for this particular value of z displacement. Interestingly, the S−Au bonding site changes from the atop site in the single adatom scenario to the hollow site on the two- or three-adatom island, which is consistent with the earlier study by Kamenetska et al.,[11] where they found a similar change in the bonding site upon tension for amide-linked junctions on Au.

Our findings are complementary to the results of ab initio molecular dynamics simulations of ref 20, which observed the formation of a monatomic Au nanowire when the molecule was bound near a step edge. Indeed, our results demonstrate that pulling-induced nanowire formation can also happen when the molecule is bonded to a flat Au(111) terrace by transferring atoms from the bulk (i.e., kink sites) or by capturing existing surface adatoms; both processes involve atomic diffusion and therefore require much longer time scales than the step edge process observed in ref 20. In the next section, we discuss possible mechanisms for the formation of pyramidal break junctions by atomic diffusion.

III.D. Model of Diffusion-Limited Break Junction Formation. On the basis of the results of our DFT calculations, we propose a diffusion-limited mechanism of break junction formation on atomically flat Au(111). Starting from a clean Au(111) surface, a surface void ("pseudo-vacancy") is generated in configurations b−c of Figure 3C by pulling the molecule and displacing the S-bonded Au atom. We illustrate the resulting configuration in Figure 6B. In the next step, the void can be filled by one of the surrounding Au atoms, converting the S-bonded Au atom into an adatom and creating a surface or bulk vacancy. The latter process becomes energetically favorable for sufficiently large displacements when the energy gain by creating an adatom (given by the difference between the black and red curves in Figure 3A) becomes as large as 1 eV, exceeding the formation energy of both bulk (0.64 eV) and surface (0.58 eV) vacancies. Upon further displacement (e.g., corresponding to point c′ in Figure 3C), an additional atom can be incorporated at the site of the molecular junction to form a bridge that links the molecule and the Au surface in the manner of Figure 6E. As discussed above in the context of Figure 5B, this process is energetically favorable by 0.3 eV, and it could likely proceed by capturing a surface adatom. As schematically shown in Figure 6F, a pyramid-shaped junction can form under the molecule via further

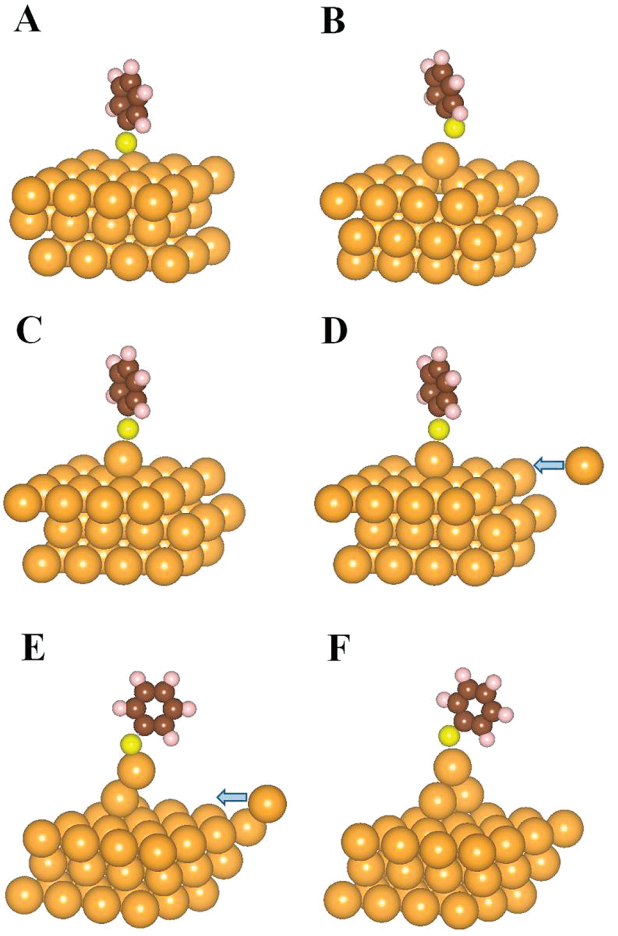

Figure 6. Schematic illustration of initial steps in the formation mechanism of a pyramidal break junction.

incorporation of diffusing adatoms. Ultimately, the size of the pyramidal junction under the molecule is limited by the balance between the energy of the Au−S bond and the surface energy penalty caused by the buildup of Au atoms under the junction.

The proposed mechanism is operational only if the pulling rate is compatible with the time scales that are required to capture diffusing adatoms. To estimate the latter, we use a simple random walk theory applied to the equilibrium density of surface adatoms

$$\rho = \frac{1}{A_0} e^{-\Delta E_{ad}/k_B T} \quad (5)$$

where ΔE_{ad} is the adatom formation energy and A_0 is the area of the (111) surface unit cell. The diffusivity of Au adatoms on Au(111) is given by

$$D = D_0 e^{-E_a/k_B T} \quad (6)$$

where D_0 is the prefactor and E_a is the activation energy for diffusion. The average time for an adatom to meet the molecule is determined from

$$1/\rho \approx 4Dt \quad (7)$$

Substituting experimental data on the surface diffusivity ($D_0 = 3.4 \times 10^{-4}$ cm^2 s^{-1}, $A_0 = 4$ Å^2, $E_a = 0.12$ eV)[32] and adatom density ($\Delta E_{ad} = 0.68$ eV) in eq 7, we obtain that the capture time t is a few seconds at $T = 300$ K.

dx.doi.org/10.1021/jp110072w |J. Phys. Chem. C XXXX, XXX, 000–000

Our work assumes a perfect Au(111) surface without herringbone reconstruction, such as encountered in the high-coverage regime of self-assembled monolayers. We note that the adatoms required by the mechanism of Figure 6 may also be supplied by the lifting of the Au(111) herringbone reconstruction, which contains an extra Au atom in the surface layer per every 22 subsurface atoms. Recent experimental investigations indicate that these extra Au atoms can be converted to adatoms upon the adsorption of the molecule.[28] We expect that this abundant source of Au adatoms can further reduce the capture time in the initial stages of break junction formation. Unfortunately, direct computational studies of the proposed mechanism on reconstructed Au(111) are currently not feasible due to the very large system size required to accommodate the reconstruction.

IV. CONCLUSIONS

We have performed first-principles calculations to study the energetics of the formation mechanism of molecular break junctions formed by benzenethiol on Au(111) under applied force. We confirm that at zero force the most favorable adsorption site for benzenethiolate is the bridge site and show that under a sufficiently high tensile force the sulfur-bonded surface Au atom can be converted into an adatom via a vacancy diffusion process. Adatom-island calculations indicate an energetic tendency to adsorb additional Au atoms from step kinks upon further junction stretching. On the basis of these results, we propose a diffusion-assisted formation mechanism of molecular break junctions for benzenethiol on Au(111). Since atomic diffusion requires a relatively long time scale, it suggests that the structure of the junction and its current−voltage characteristics could vary significantly with the stretching rate, which should be slower than typical adatom capture rates to prevent breakage of the molecular junction. Systematic experimental studies of the temperature dependence of the molecular break junction formation under different stretching rates could be used to verify the proposed model.

AUTHOR INFORMATION

Corresponding Author

*E-mail: vidvuds@ucla.edu.

ACKNOWLEDGMENT

This work was supported as part of the Molecularly Engineered Energy Materials (MEEM), an Energy Frontier Research Center funded by the U.S. Department of Energy, Office of Science, Office of Basic Energy Sciences under Award Number DE-SC0001342. This research used resources of the National Energy Research Scientific Computing Center (NERSC).

REFERENCES

(1) Reed, M. A. *Science* **1997**, *278*, 252.
(2) Elbing, M.; Ochs, R.; Koentopp, M.; Fischer, M.; von Hanisch, C.; Weigend, F.; Evers, F.; Weber, H. B.; Mayor, M. *Proc. Natl. Acad. Sci. U.S.A.* **2005**, *102*, 8815.
(3) Kiguchi, M.; Tal, O.; Wohlthat, S.; Pauly, F.; Krieger, M.; Djukic, D.; Cuevas, J. C.; van Ruitenbeek, J. M. *Phys. Rev. Lett.* **2008**, *101*, 046801.
(4) Ratner, M. *Nature* **2005**, *435*, 575.
(5) Joachim, C.; Ratner, M. A. *Proc. Natl. Acad. Sci. U.S.A.* **2005**, *102*, 8801.
(6) Davis, W. B.; Svec, W. A.; Ratner, M. A.; Wasielewski, M. R. *Nature* **1998**, *396*, 60.
(7) Guo, X. F.; Small, J. P.; Klare, J. E.; Wang, Y. L.; Purewal, M. S.; Tam, I. W.; Hong, B. H.; Caldwell, R.; Huang, L. M.; O'Brien, S.; Yan, J. M.; Breslow, R.; Wind, S. J.; Hone, J.; Kim, P.; Nuckolls, C. *Science* **2006**, *311*, 356.
(8) Reddy, P. *Science* **2007**, *315*, 1568.
(9) Nitzan, A.; Ratner, M. A. *Science* **2003**, *300*, 1384.
(10) Xiao, X. Y. *Nano Lett.* **2004**, *4*, 267.
(11) Kamenetska, M.; Koentopp, M.; Whalley, A. C.; Park, Y. S.; Steigerwald, M. L.; Nuckolls, C.; Hybertsen, M. S.; Venkataraman, L. *Phys. Rev. Lett.* **2009**, *102*, 126803.
(12) Li, Z. *Phys. Rev. B* **2007**, *76*, 035415.
(13) Basch, H.; Cohen, R.; Ratner, M. A. *Nano Lett.* **2005**, *5*, 1668.
(14) Ramachandran, G. K.; Hopson, T. J.; Rawlett, A. M.; Nagahara, L. A.; Primak, A.; Lindsay, S. M. *Science* **2003**, *300*, 1413.
(15) Wang, G. M.; Sandberg, W. C.; Kenny, S. D. *Nanotechnology* **2006**, *17*, 4819.
(16) Love, J. C.; Estroff, L. A.; Kriebel, J. K.; Nuzzo, R. G.; Whitesides, G. M. *Chem. Rev.* **2005**, *105*, 1103.
(17) Mazzarello, R.; Cossaro, A.; Verdini, A.; Rousseau, R.; Casalis, L.; Danisman, M. F.; Floreano, L.; Scandolo, S.; Morgante, A.; Scoles, G. *Phys. Rev. Lett.* **2007**, *98*, 016102.
(18) Cossaro, A.; Mazzarello, R.; Rousseau, R.; Casalis, L.; Verdini, A.; Kohlmeyer, A.; Floreano, L.; Scandolo, S.; Morgante, A.; Klein, M. L.; Scoles, G. *Science* **2008**, *321*, 943.
(19) Maksymovych, P.; Yates, J. T. *J. Am. Chem. Soc.* **2008**, *130*, 7518.
(20) Kruger, D.; Fuchs, H.; Rousseau, R.; Marx, D.; Parrinello, M. *Phys. Rev. Lett.* **2002**, *89*, 186402.
(21) Kresse, G.; Hafner, J. *Phys. Rev. B* **1993**, *47*, 558.
(22) Perdew, J. P.; Burke, K.; Ernzerhof, M. *Phys. Rev. Lett.* **1996**, *77*, 3865.
(23) Vanderbilt, D. *Phys. Rev. B* **1990**, *41*, 7892.
(24) Quek, S. Y.; Biener, M. M.; Biener, J.; Bhattacharjee, J.; Friend, C. M.; Waghmare, U. V.; Kaxiras, E. *J. Phys. Chem. B* **2006**, *110*, 15663.
(25) Pimpinelli, A.; Villain, J. *Phys. Crystal Growth* **1997**, *1*, 4.
(26) Schreiber, F. *Prog. Surf. Sci.* **2000**, *65*, 151.
(27) Nara, J.; Higai, S.; Morikawa, Y.; Ohno, T. *J. Chem. Phys.* **2004**, *120*, 6705.
(28) Nenchev, G.; Diaconescu, B.; Hagelberg, F.; Pohl, K. *Phys. Rev. B* **2009**, *80*, 081401.
(29) Yu, M.; Bovet, N.; Satterley, C. J.; Bengio, S.; Lovelock, K. R. J.; Milligan, P. K.; Jones, R. G.; Woodruff, D. P.; Dhanak, V. *Phys. Rev. Lett.* **2006**, *97*.
(30) Grandbois, M.; Beyer, M.; Rief, M.; Clausen-Schaumann, H.; Gaub, H. E. *Science* **1999**, *283*, 1727.
(31) Huang, W. J.; Sun, R.; Tao, J.; Menard, L. D.; Nuzzo, R. G.; Zuo, J. M. *Nat. Mater.* **2008**, *7*, 308.
(32) Ferrando, R. *Surf. Sci.* **1995**, *333*, 920.